TISSUE ENGINEERING: Part A
Volume 18, Numbers 5 and 6, 2012

DOI: 10.1089/ten.tea.2011.0349

Granule Size–Dependent Bone Regenerative Capacity of Octacalcium Phosphate in Collagen Matrix

Yuji Tanuma, D.D.S., Ph.D.,[1,2,*] Takahisa Anada, Ph.D.,[2,*] Yoshitomo Honda, D.D.S., Ph.D.,[2]
Tadashi Kawai, D.D.S., Ph.D.,[1] Shinji Kamakura, D.D.S., Ph.D.,[3]
Seishi Echigo, D.D.S., Ph.D.,[1] and Osamu Suzuki, Ph.D.[2]

The present study was designed to determine whether the osteoconductivity of octacalcium phosphate–collagen (OCP/Col) composite can be improved by controlling the granule size of OCP. The granules of synthetic OCP, with diameters in the range of 53 to 300, 300 to 500, and 500 to 1000 μm, were used as an inorganic source of composite materials mixed with atelo-Col. After vacuum dehydrothemal treatment, OCP/Col disks were implanted into critical-sized calvaria defects in Wistar rats for 4, 8, and 12 weeks and examined radiographically, histologically, histomorphometrically, and histochemically. The materials were characterized according to mercury intrusion porosimetry and scanning electron microscopy. X-ray diffraction was performed before and after implantation. The dissolution of OCP crystals in a Col matrix was determined by immersing OCP/Col disks in a culture medium. OCP/Col had a constant pore size (~30 μm) regardless of OCP granule size. OCP in the Col matrix tended to convert to hydroxyapatite (HA) during the implantation. OCP/Col with the smallest granules of OCP enhances both bone regeneration and biodegradation the most through tartrate-resistant acid phosphatase (TRAP)-positive osteoclastic cellular resorption of OCP granules. The smallest OCP granules in the Col matrix showed the highest dissolution and had the greatest potential to form HA. The results indicated that the size of the included OCP granules can controll the osteoconductivity of OCP/Col. The overall results suggest that the physicochemical property of OCP crystals is a factor that determines the bone regenerative capacity of OCP/Col in critical-sized calvaria large bone defects in rats.

Introduction

One of the characteristics of biomaterials used at load-bearing sites as a nonresorbable synthetic bone substitute is high strength,[1] although there is consensus that bone substitute materials should provide a framework for continuous bone resorption and bone deposition[2] because such biodegradable materials are integrated into a natural bone remodeling process caused by the resorption of the existing bone matrix together with the implanted materials by osteoclasts and the deposition of new bone matrix by osteoblasts.[2] Much attention has been given to the investigation and development of various biodegradable calcium phosphate ceramics *in vivo*, such as beta-tricalcium phosphate (β-TCP),[3,4] with an adjusted level of bioactivity and the capacity for new bone formation, but no ideal material condition has yet been found.

The solubility of calcium phosphates is a factor affecting their possible order of dissolving in physiological environments.[5] β-TCP is more soluble than hydroxyapatite (HA) in a neutral condition.[5,6] HA has the least solubility of calcium phosphates in that condition and is nonresorbable *in vivo* if it is sintered and has a stoichiometric formula with a calcium:phosphate (Ca/P) molar ratio of 1.67,[3,7] but the stability of HA decreases if a carbonate ion is included in its structure.[8] The physicochemical properties of HA and β-TCP (porosity, shape, and size), which could be associated with the apparent solubility of these materials, have been found to influence the outcome of *de novo* bone formation in bone defects.[9,10] Osteoclast-like cells resorb β-TCP,[4, 10] carbonate-containing HA,[11] and HA with nanoscale[12] *in vivo*, facilitating bone regeneration by these materials in bone defects.

Octacalcium phosphate (OCP), thought to be a precursor to HA[13] that is biodegradable *in vivo*,[14,15] is more soluble than β-TCP in neutral solutions.[5] It was recently found that OCP is capable of inducing osteoclast formation from the co-culturing of osteoblasts and bone marrow cells, through the increase of expression of osteoblasts of osteoclast-inducing

Divisions of [1]Oral Surgery, [2]Craniofacial Function Engineering, Graduate School of Dentistry, Tohoku University, Sendai, Japan.
[3]Division of Bone Regenerative Engineering Laboratory, Graduate School of Biomedical Engineering, Tohoku University.
*These authors contributed equally to this work.

factor RANKL, even in the absence of vitamin D_3, a regulator of osteoclastogenesis.[16] Furthermore, OCP enhances osteoblast differentiation *in vitro*.[17-19] Our previous study showed that OCP, if synthesized under specific conditions, is not only more resorbable than sintered β-TCP in bone defects, because of osteoclastic cellular resorption, but is also more osteoconductive than β-TCP or stoichiometric and nonstoichiometric HA.[20-22] The osteoconductive and biodegradable characteristics of OCP have also been reproduced in the form of a composite with natural polymers, such as Col[23] and alginate.[24] From these findings, we hypothesized that OCP could be used as a source material for various scaffold materials, such as polymers used in tissue engineering, making it possible to include OCP in the bone remodeling process.

There is general consensus that the type of scaffold materials,[25] composition (inorganic versus organic),[26] biodegradability, cell-adhesive property,[25] pore size, and porosity[27] control the bone regenerative property of the materials, including calcium phosphate materials. Bone regeneration has been demonstrated to be enhanced with increasing the granule size of OCP, which is accompanied by the augmented appearance of the osteoclasts around them.[28] The effects of OCP mixing with Col[23] and the dose[29] in the form of granules of OCP in the Col sponge have been examined, but the effect of the size of OCP granules in a Col matrix has not been examined. In this study, we investigated the granule size of OCP and how it affects the bone regenerative and biodegradable properties of the OCP/Col composites in critical-sized rat calvaria bone defects, if the composites are prepared under a constant condition, which ensures that the composite property is relatively constant except for the granule size of OCP.

Materials and Methods

Preparation of OCP, Col disks, and OCP/Col disks

OCP was prepared by mixing calcium and phosphate solutions as described previously.[22] The granules, consisting of an OCP crystal aggregate, were prepared from OCP precipitates by passing through a standard testing sieve. Granules with diameters ranging from 53 to 300 μm, 300 to 500 μm, and 500 to 1,000 μm were used. The sieved OCP granules were sterilized by heating at 120°C for 2 hours. As shown previously, such heating does not affect the physical properties, such as the crystalline structure or specific surface area of OCP granules,[30,31] although it has been reported that temperatures greater than 100°C induce a gradual collapse of the OCP structure due to dehydration.[32,33] A 1% solution of Col was purchased from NMP Collagen PS (Nippon Meat Packers, Tsukuba, Ibaraki, Japan). The solution was adjusted to pH 7.4 to form a gel of Col fibrils. The Col solution was then condensed by centrifugation. The Col suspension at a concentration of 3% was prepared from the condensed Col suspension. OCP granules were added to the concentrated Col and mixed. The weight percentage of OCP in OCP/Col was 77%. This OCP/Col mixture was then lyophilized, and the disks were molded (9-mm diameter, 1 mm thick). The molded OCP/Col underwent dehydrothermal treatment (DHT; 120°C,150°C, or 180°C, 24 hours) in a vacuum drying oven (DP32, Yamato Scientific, Tokyo, Japan) and was then sterilized using electron beam irradiation (5 kGy). The Col disks as the control material were prepared with identical treatments.

Characterization of OCP/Col disks

OCP/Col disks were characterized using X-ray diffraction (XRD). The XRD patterns were recorded using step scanning at 0.05° intervals from 3.0° to 60.0°, with Cu Kα X-rays on a diffractometer (Mini Flex, Rigaku Electrical Co., Ltd., Tokyo, Japan) at 30 kV, 15 mA. The 2θ range measured included the primary peak (100) of OCP at 4.7°. Joint Committee for Powder Diffraction Standard (JCPDS) number 26-1056A9 for OCP and 9-432 for HA were used to identify their crystalline phases. The porosity was determined according to mercury intrusion porosimetry (PoreMaster60GT, analyzed by KN Lab Analysis, Hyogo, Japan). The morphology of OCP/Col disks was examined using a JEOL analytical scanning electron microscope JSM-6390LA (Tokyo, Japan) operating at an accelerating voltage of 10 kV. Gold sputtering was performed before the observation.

Implantation of OCP/Col or Col in rat calvaria bone defect

Twelve-week-old male Wistar rats (SLC, Hamamatsu, Shizuoka, Japan) were used. The principles of laboratory animal care and national laws were followed. The Animal Research Committee of Tohoku University approved all procedures.

The experimental rats were anesthetized with intraperitoneal sodium pentobarbital (50 mg/kg) supplemented by ether inhalation. A skin incision was made aseptically along the bilateral temporal line and the middle of the forehead, and the dissection was continued to the calvarium. The periosteum of the calvarium was ablated, and a full-thickness standardized trephine defect, 9 mm in diameter, was made in the calvarium under continuous saline buffer irrigation. Extreme care was exercised to avoid injury to the midsagittal blood sinus and dura mater. OCP/Col or Col disks were implanted into the trephine defect. As a negative control, untreated animals were processed in the same way except that nothing was implanted after the defects were created. After the defects were treated, the ablated periosteum was repositioned and the skin sutured. Five rats in each of the OCP/Col-treated, Col-treated, and untreated groups were anesthetized and sacrificed for the tissue fixation at 4, 8, and 12 weeks after implantation as described below.

Radiographic analysis

The rats were anesthetized by intraperitoneal sodium pentobarbital (50 mg/kg), and sacrificed with 4% paraformaldehyde in 0.1M PBS (pH 7.4) by perfusion through the aorta for the tissue fixation. The implants were resected together with the surrounding bones and tissues and kept in the same fixative overnight at 4°C. The specimens were radiographed using a microradiography unit (Softex CMR Unit, Softex, Tokyo, Japan) with X-ray film (FR, Fuji Photo Film, Tokyo, Japan) under standardized conditions (20 kV, 5 mA, 1 minute) under which OCP showed no radiopacity.

Tissue preparation

After the radiographic analyses, the samples were decalcified in 10% ethylenediaminetetraacetic acid in a 0.01M phosphate buffer (pH 7.4) for 2 to 4 weeks at 4°C. The

samples were dehydrated in a graded series of ethanol and embedded in paraffin. The center of the defect was extracted and sectioned coronally at a thickness of 5 μm. The sections were stained with hematoxylin and eosin and tartrate-resistant acid phosphatase (TRAP), and photographs were taken using a photomicroscope (Leica DFC300 FX, Leica Microsystems Japan, Tokyo, Japan).

Quantitative micrograph analysis

Light micrographs of the sections stained with hematoxylin and eosin were used for histomorphometric measurements. Photographs projecting the overall defect were taken of each specimen. The percentage of newly formed bone in the defect (n-Bone%) was calculated as the area of newly formed bone per area of the defect originally created by trephination × 100. Likewise, the percentage of remaining OCP in the defect (r-Imp%) was calculated as the area of remaining OCP per area of the defect originally created by trephination × 100. The n-Bone% and r-Imp% were quantified on a computer using Scion Image public domain software (Scion Corporation, Frederick, MD).

XRD of implanted OCP

The OCP implanted in the rat calvaria was examined for XRD. The OCP/Col implanted for 12 weeks was collected from rat calvarial bone defects of two to four rats using tweezers to exclude as much of the soft tissue around the implanted OCP as possible. The OCP/Col was immediately dipped in PBS and deionized water and then in absolute alcohol to dry. The OCP/Col was ground using a mortar and pestle and examined for powder XRD under the same conditions used for the characterization of OCP as reported above.

Dissolution estimation of OCP/Col disks immersed in a culture medium

The concentration of calcium ions (Ca^{2+}) and inorganic phosphate ions (Pi) in an alpha minimal essential medium (αMEM) was determined quantitatively using Calcium E and Phosphor C tests (Wako Pure Chemical Industries, Osaka, Japan), respectively. Ten milligrams of OCP/Col disks was immersed in 750 μL of αMEM for 3 days at 37°C in a 5% carbon dioxide environment. The supernatants after the immersion were collected for Ca^{2+} and Pi quantitative analyses.

Degree of supersaturation of media after immersing OCP/Col composites

Degree of supersaturation (DS) of αMEM and after immersing OCP/Col composites and Col disks was calculated to estimate the dissolution of OCP granules with respect to OCP, HA, and dicalcium phosphate dihydrate (DCPD) in the media. DS can be expressed by dividing the ionic product by the solubility product in objective calcium phosphate compound and stands for saturation when the value is 1. DS is usually calculated using the analytical results of [Ca], [Mg], [Na], [K], [P], [Cl], and [F] and the pH value in conjunction with the three mass balance equations for [Ca], [P], and [Mg], according to previous reports.[34-36] The calculation also assumed the presence of HCO^{3-} in the fluid. The ion pairs considered were CaH_2PO^{4+}, $CaHPO_4^0$, $MgHPO_4^0$, $CaHCO^{3+}$, and $MgHCO^{3+}$. DS was defined in terms of their mean ionic activity product with respect to OCP, HA, and DCPD. In the present calculation, the concentration of Ca^{2+} and Pi obtained using chemical analyses was used. Ionic strength with 150mM as Na^+ was assumed. pH 7.4 and physiologic partial pressure 1.86% in carbonate were used for the calculation. Other species, such as Mg^{2+} and F^-, were assumed to be approximately 0. The solubility product constants used were 2.63×10^{-60} for HA[37] and 1.05×10^{-47} for OCP.[38]

Statistical analysis

Results were expressed as means ± standard deviations (SDs). All cellular experiments were performed at least three times and showed reliable reproducibility. Statistical analysis was performed for all of the cellular and histomorphometric experiments using commercial software (Ekuseru-Toukei 2006, Social Survey Research Information, Tokyo, Japan). One-way analysis of variance (ANOVA) was used to compare the means between groups. If the ANOVA was significant, Tukey's multiple comparison analysis was used as a *post hoc* test.

Results

XRD patterns of OCP/Col, OCP, and Col

We prepared OCP/Col with OCP granules 300 to 500 μm in diameter and processed it with different temperatures of DHT (120°C, 150°C, or 180°C). The peaks diffracted from OCP/Col 120°C, OCP/Col 150°C, OCP/Col 180°C, OCP, and Col are shown in Figure 1. Although XRD patterns obtained in OCP/Col disks contained the characteristic (100) reflection of OCP at 2θ = 4.7°, corresponding well with those expected from the OCP structure,[39] they showed the structural changes of OCP. OCP in OCP/Col revealed the partial collapse of the (100) peak with a reduction of the (700) peak around 33.6° due to DHT. OCP/Col had an HA-like XRD pattern but the characteristics of OCP.

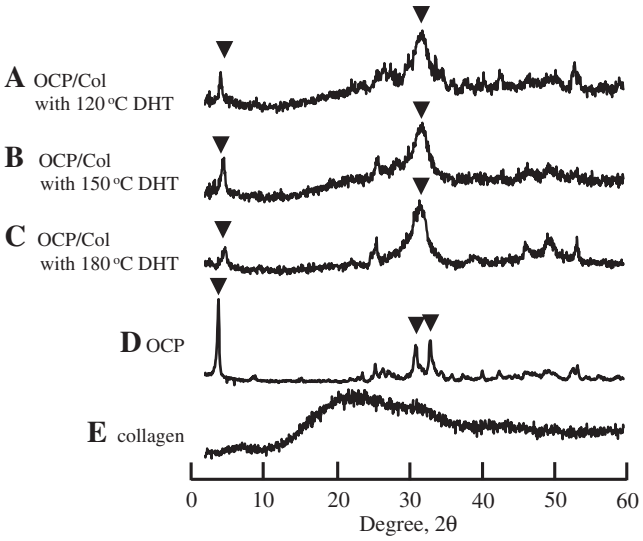

FIG. 1. X-ray diffraction patterns of **(A)** octacalcium phosphate (OCP)/collagen (Col) with 120°C dehydrothermal treatment (DHT), **(B)** OCP/Col with 150°C DHT, **(C)** OCP/Col with 180°C DHT, **(D)** OCP, and **(E)** Col. The size of the OCP granules was 300-500 μm. ▼, OCP reflection.

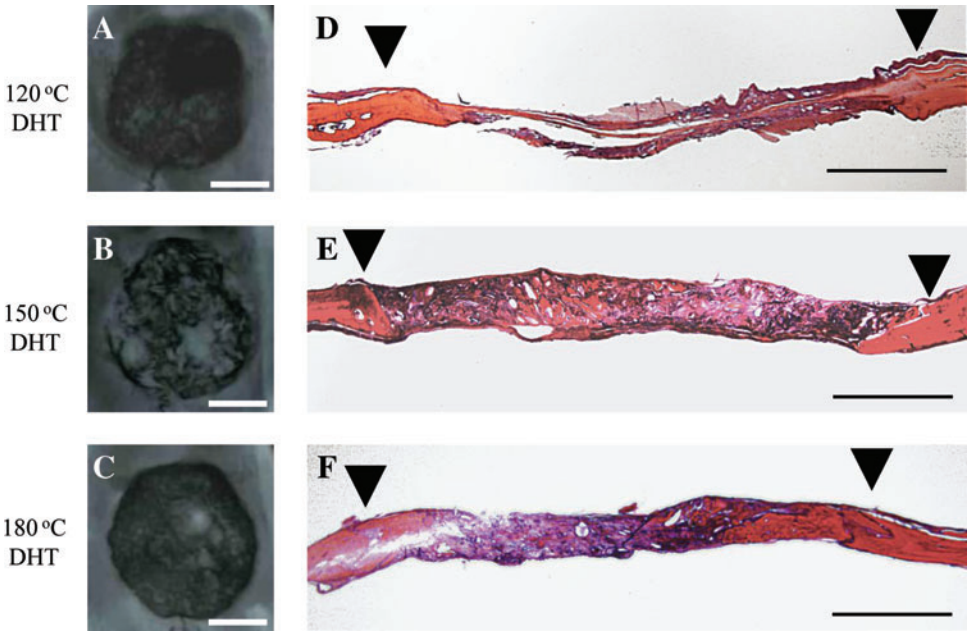

FIG. 2. Radiographic examination and histological overview of the implants in week 12. **(A, D)** OCP/Col with 120°C DHT, **(B, E)** OCP/Col with 150°C DHT, and **(C, F)** OCP/Col with 180°C DHT. ▼, defect margin. Bars = 4 mm (**A–C**), 2 mm (**D–F**). Color images available online at www.liebertonline.com/tea

Bone regeneration of OCP/Col with different temperature of DHT

We previously reported that DHT during the fabrication of OCP/Col influences bone regeneration by OCP/Col.[40] New bone formation by OCP/Col with DHT was significantly higher than that without DHT,[40] although it is unclear whether the temperature of the DHT is optimized with regard to the osteoconductive characteristics of OCP/Col. Bone regeneration by the implantation of OCP (300-500 μm)/Col with different DHT (120°C, 150°C, and 180°C) was compared. The results of the radiographic examination are shown in Figure 2 (A-C). At week 12, there was moderate radiopacity in the defect implanted with OCP/Col with 120°C DHT (Fig. 2A). In OCP/Col with 180°C DHT (Fig. 2C), the radiopacity was higher than that in OCP/Col with 120°C DHT, but the area of radiopacity was smaller than the defect. In OCP/Col with 150°C DHT (Fig. 2B), a larger area of thorn-like radiopacity amalgamated and condensed.

An overview of histological sections at week 12 is shown in Figure 2D-F. New bone formation of OCP/Col with 120°C DHT was limited to the defect margin and around the implanted OCP (Fig. 2D). In OCP/Col with 180°C DHT (Fig. 2F), newly formed bone was observed sporadically in the defect. The area of newly formed bone was larger than that with OCP/Col with 120°C DHT. In OCP/Col with 150°C DHT (Fig. 2E), newly formed bone was observed throughout the defect and surrounding the remaining OCP. The area of newly formed bone of OCP/Col with 150°C DHT was larger than that in other samples.

Radiographic examination of OCP/Col with different granule size of OCP

As described above, the OCP/Col with 150°C DHT enhanced bone regeneration more than that with 120°C or 180°C DHT. Therefore, OCP/Col with 150°C DHT was evaluated further. The size effect of OCP granules (53-300 μm, 300-500 μm, or 500-1,000 μm) in Col was examined. The results of the radiographic examination are shown in Figure 3. In OCP/Col, thorn-like radiopaque masses were scattered throughout the defect in week 4 and condensed in weeks 8 and 12, and newly formed bone was observed in a large area of the defect. In particular, in 53- to 300-μm OCP/Col, the amalgamated radiopacity was more condensed and became larger than that of other samples. In Col, isolated pudgy radiopacities were scattered throughout the defect. In untreated defects, radiopacity was observed along the defect margins.

Histological examination of OCP/Col with different granule size of OCP

An overview of the histological sections (Fig. 4) showed that bone regeneration in the Col-treated group and the untreated control was limited to the margin of the defect, and most of the defect was filled with fibrous connective tissue. In OCP/Col, newly formed bone in the defect became abundant in week 12. The area of newly formed bone of 53- to 300-μm OCP/Col was the largest of the samples.

Histomorphometric examination

Histomorphometric findings regarding n-Bone% are shown in Figure 5. By week 4, mean n-Bone% ± SD in the 500- to 1,000-μm OCP/Col-treated, 300- to 500-μm OCP/Col-treated, 53- to 300-μm OCP/Col-treated, Col-treated, and untreated groups was 16.3 ± 3.9, 17.9 ± 3.3, 23.0 ± 3.2, 6.4 ± 1.6, and 6.0 ± 1.6, respectively. A significant difference was observed between the 53- to 300-μm OCP/Col-treated and other groups. By week 8, the mean n-Bone% ± SD in 500- to 1000-μm OCP/Col-treated, 300- to 500-μm OCP/Col-treated, 53- to 300-μm OCP/Col-treated, Col-treated, and untreated groups was 37.3 ± 2.2, 38.0 ± 2.0, 53.2 ± 2.7, 15.3 ± 3.6, and 9.8 ± 3.3, respectively. A significant difference was observed between the 53- to 300-μm OCP/Col-treated and other groups. By week 12, the mean n-Bone% ± SD in the 500- to 1,000-μm OCP/Col-treated, 300- to 500-μm OCP/Col-treated, 53- to 300-μm OCP/Col-treated, Col-treated, and untreated groups was 56.1 ± 2.8, 53.7 ± 3.1, 65.5 ± 3.1,

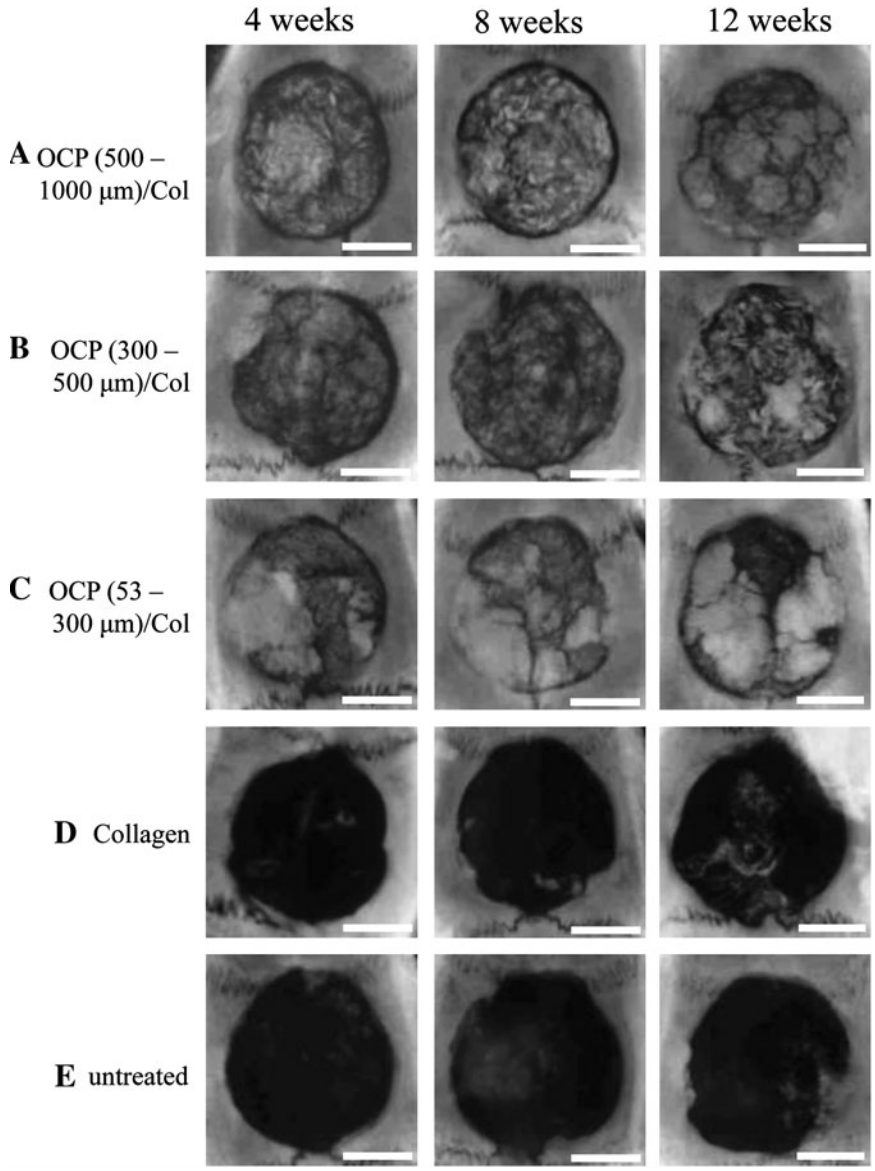

FIG. 3. Radiographs of rat calvarial defects with implantation of **(A)** 500- to 1,000-μm OCP/Col, **(B)** 300- to 500-μm OCP/Col, **(C)** 53- to 300-μm OCP/Col, and **(D)** Col; **(E)** untreated control. Dehydrothermal treatment was 150°C. Bars = 4 mm.

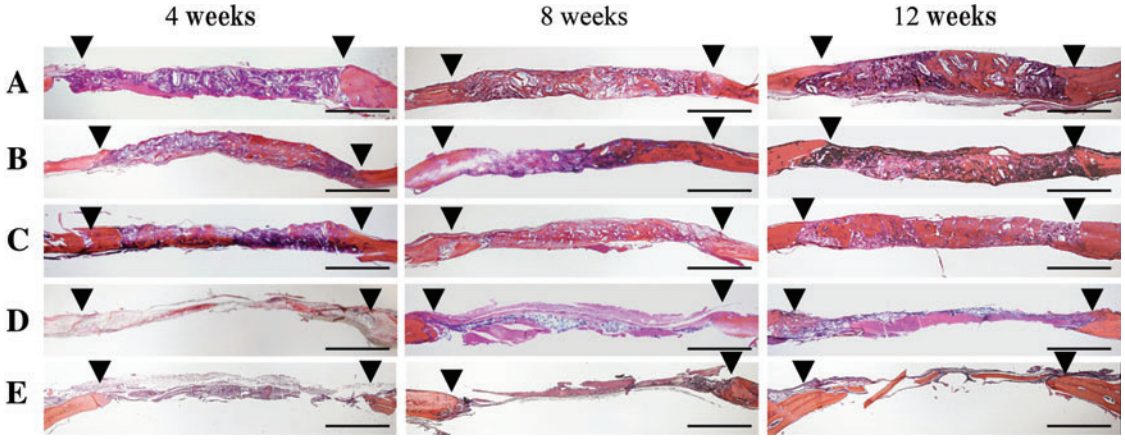

FIG. 4. Overview of the sections stained with hematoxylin and eosin: **(A)** 500- to 1,000-μm OCP/Col, **(B)** 300- to 500-μm OCP/Col, **(C)** 53- to 300 μm OCP/Col, **(D)** Col, and **(E)** untreated control. The implantation terms were 4, 8, and 12 weeks long. Dehydrothermal treatment was 150°C. ▼, defect margin. Bars = 2 mm. Color images available online at www.liebertonline.com/tea

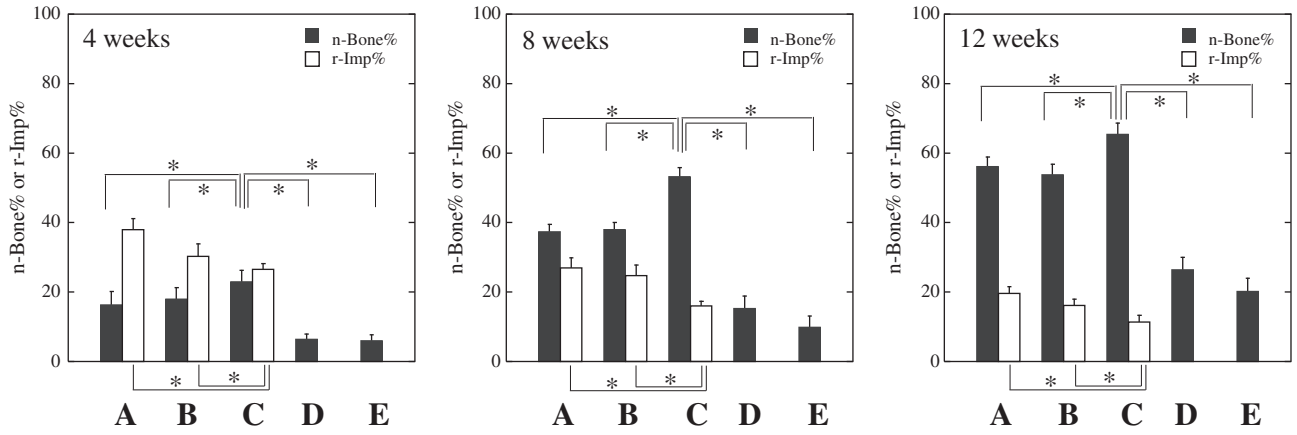

FIG. 5. Quantitative analysis of percentage of new bone in the defect (n-Bone%) and remaining implant (r-Imp%). **(A)** 500- to 1,000-μm OCP/Col, **(B)** 300- to 500-μm OCP/Col, **(C)** 53- to 300-μm OCP)/Col, **(D)** Col, and **(E)** untreated control. Data are means ± standard deviations. *$p < 0.01$.

26.4 ± 3.6, and 20.2 ± 3.8, respectively. A significant difference was observed between the 53- to 300-μm OCP/Col-treated and other groups.

Histomorphometric findings regarding r-Imp% are shown in Figure 5. By week 4, the mean r-Imp% ± SD in the 500- to 1,000-μm OCP/Col-treated, 300- to 500-μm OCP/Col-treated, and 53- to 300-μm OCP/Col-treated groups was 38.0 ± 3.1, 30.3 ± 3.6, and 26.5 ± 1.7, respectively. A significant difference was seen between OCP/Col composites. By week 8, the mean r-Imp% ± SD in the 500- to 1,000-μm OCP/Col-treated, 300- to 500-μm OCP/Col-treated, and 53- to 300-μm OCP/Col-treated groups was 26.9 ± 3.0, 24.7 ± 3.1, and 16.0 ± 1.4, respectively. A significant difference was seen between OCP/Col composites. By week 12, the mean r-Imp% ± SD in the 500- to 1,000-μm OCP/Col-treated, 300- to 500-μm OCP/Col-treated, and 53- to 300-μm OCP/Col-treated groups was 19.6 ± 1.9, 16.1 ± 1.9, and 11.4 ± 1.9, respectively. A significant difference was seen between OCP/Col composites.

TRAP staining

Representative TRAP staining at 4 weeks is shown in Figure 6. TRAP-positive multinucleated giant cells (MNGCs) were observed in close association with OCP granules, indicating that TRAP-positive osteoclast-like cells directly resorb OCP granules within the Col matrix. Sparse TRAP-positive cells were seen within the implant, in particular around 53- to 300-μm OCP granules (Fig. 6c, F).

Structural changes of OCP in vivo

Figure 7 shows the XRD patterns of the OCP/Col before (Fig. 7C, E, G) and after (Fig. 7B, D, F) implantation in rat calvarial defects. The structure of OCP tended to convert to

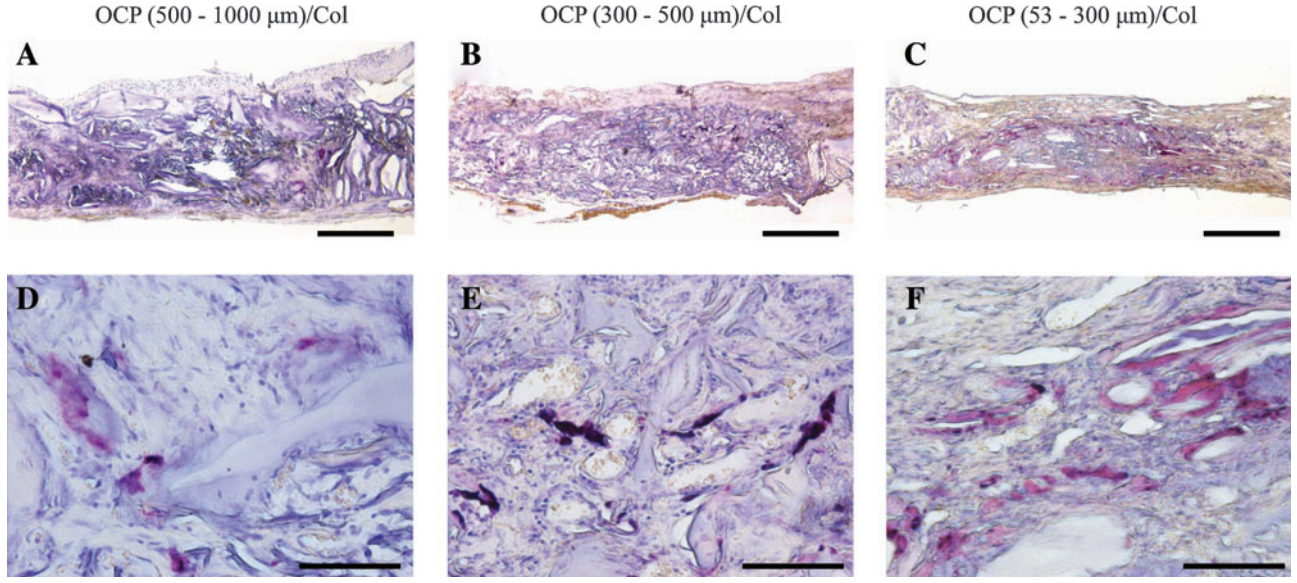

FIG. 6. Detection of tartrate-resistant acid phosphatase (TRAP)-positive multinucleated giant cells (MNGCs) around OCP granules. TRAP staining at 4 weeks: **(A, D)** 500- to 1,000-μm OCP/Col, **(B, E)** 300- to 500-μm OCP/Col, and **(C, F)** 53- to 300-μm OCP/Col. Bars = 500 μm **(A,B,C)**, 200 μm **(D,E,F)**. Color images available online at www.liebertonline.com/tea

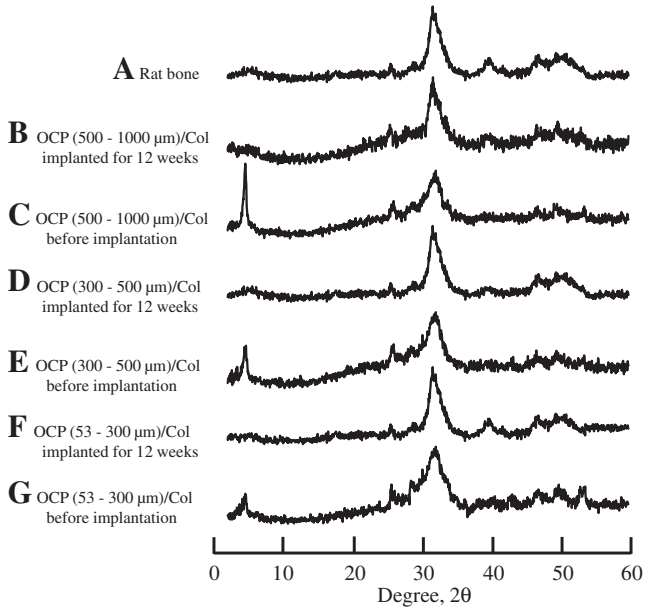

FIG. 7. X-ray diffraction patterns of **(A)** rat bone and **(B)** 500- to 1,000-μm OCP/Col implanted into rat calvarial defects at 12 weeks, **(C)** 500- to 1,000-μm OCP/Col before implantation, **(D)** 300- to 500-μm OCP/Col implanted, **(E)** 300- to 500-μm OCP)/Col before implantation, **(F)** 53- to 300-μm OCP/Col implanted, and **(G)** 53- to 300-μm OCP/Col before implantation.

that of HA with a reduction in (100) reflection intensity. The results confirmed that OCP in a Col matrix tended to convert to an apatite structure by implantation into rat bone; these changes were identical to the structural changes observed by implantation into rat calvaria,[19] mouse calvaria,[22] and subcutaneous tissue.[30]

Characterization of OCP/Col disks

Figure 8 shows scanning electron micrographs of the OCP/Col disks. The granules in the Col matrix showed an irregular morphology consisting of an aggregate form of OCP crystals (Fig. 8a-C). The pore size distributions from the mercury porosimetry data are shown in Figure 9. All disks were porous and had pore size distributions with almost the same median pore sizes ($\sim$30 μm). The scanning electron micrograph figures have structures that coincide with the mercury porosimetry pore size distribution (Fig. 8d-F).

Dissolution of OCP granules in media

Figure 10 shows the results of chemical analyses of the supernatants of the OCP/Col after 3 days of incubation with αMEM at 37°C. The Ca^{2+} concentration of the supernatant of the OCP/Col was less than that of Col and control (Fig. 10A). Conversely, the Pi concentration of the supernatant of the OCP/Col was greater than those of Col and control and was greater with smaller size of the OCP granules (Fig. 10B). Table 1 shows the DS of the media before and after the immersion of OCP/Col composites. The results showed that DS in all media examined were supersaturated with respect to HA and slightly supersaturated with respect to OCP but undersaturated with respect to DCPD. DS of Col was compatible with that of the control (medium without immersing the materials) and higher than those of OCP/Col composites with respect to HA and OCP. DS of OCP/Col (53-300 μm) was somewhat smaller than those of 300- to 500-μm and 500- to 1,000-μm OCP/Col with respect to HA and OCP, indicating that 53- to 300-μm OCP granules in Col matrix had a higher potential to dissolve and tended to form HA and possibly OCP.

Discussion

The present study provides evidence that the granule size of OCP dispersed in a Col matrix greatly affects the capability of bone regeneration of OCP/Col and the degree of resorption of this composite material. The OCP/Col with the smallest OCP granules (53-300 μm) enhanced the bone regeneration rate in a rat critical-sized calvaria defect more than those with OCP granules with larger ranges (300-500 and 500-1,000 μm). The resorption of OCP/Col was also more enhanced in the composite including the smallest OCP granules (53-300 μm) than in other OCP/Col composites with larger OCP granules. The thermal dehydration of OCP/Col under vacuum conditions, a measure to cross-link atelo-Col fibrils,[41] reconfirmed that the bone regeneration is supported most efficiently if the treatment is performed under certain conditions.[40] The present study focused on an OCP/Col composite treated at 150°C, which revealed higher bone regenerative capability. The amount of cross-linking was greater with higher dehydrothermal temperature.[41] The extent of the cross-linking in Col may affect the material characteristics[42] and regulate the capacity of bone regeneration by the present composite materials. The OCP/Col materials were well characterized to interpret the biological response in a rat critical-sized calvaria defect. The OCP structure gradually collapses if heated in air from 150°C to 200°C,[32,33] but the present DHT, which was heated to 180°C under vacuum conditions, did not induce full decomposition of the OCP structure, at least by the estimation in XRD. The X-ray pattern of OCP in the Col matrix became somewhat broader with smaller granule size, which could be due to the decrease in the crystal orientation within the Col matrix. The mercury intrusion porosimetry of the OCP/Col showed that the pore distribution was relatively homogenous ($\sim$30 μm) regardless of the granule size of OCP. The material characterization indicated that the biological responses of OCP/Col can be evaluated as a function of the granule size of OCP under which other parameters of the material are relatively constant.

A radiograph of the OCP/Col implantation showed that radiopacity progressively increases sporadically and the calcified matter fuses throughout the defect time dependently. Our previous studies indicated that bone formation is initiated from OCP granule surface,[22,30,43] although bone formation is also observed from the margin of the defect.[19,43] Bone formation is not induced if OCP is implanted in mouse abdominal subcutaneous tissue near fascia.[30] The present histological findings supported the observation that OCP granules work as a nucleation site for bone regeneration. The OCP granules in Col matrix were detected as hematoxylinophilic substances, which have been confirmed to stem from the accumulation of matrix proteins,[22] including circulating serum proteins,[30] within the space formed by each OCP crystal. Previous studies suggested that bone

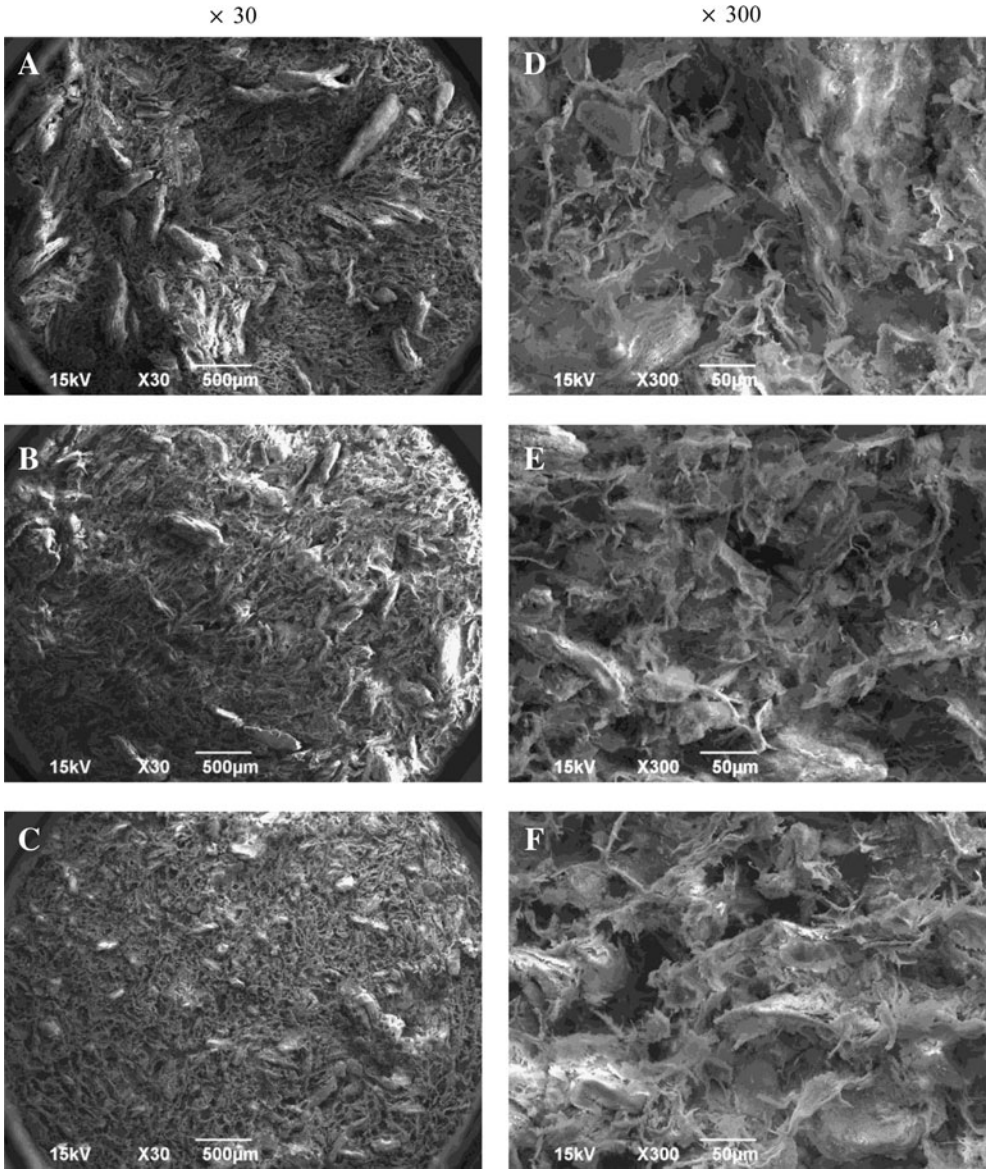

FIG. 8. Scanning electron micrographs of OCP/Col disks. **(A, D)** 500- to 1,000-μm OCP/Col, **(B, E)** 300- to 500-μm OCP/Col, and **(C, F)** 53- to 300-μm OCP/Col. Bars = 500 μm **(A,B,C)**, 50 μm **(D,E,F)**.

regeneration starts from the surface of the structure composed of OCP crystals and matrix proteins,[22] which is formed by implanting the OCP granules into bone tissue. Although Col is a cell-attaching biological molecule,[44] the present Col disks did not result in greater bone formation than OCP/Col. The results suggest that the major contribution in enhancing bone formation may stem from the capacity of OCP crystals to stimulate host osteoblastic cells to differentiate.[17,19] The fact that the capacity of bone regeneration differs depending on granule size suggests the following mechanisms; a reduction in the granule size within the unit volume of the Col matrix increases the nucleation site for new bone and some physicochemical change in relation to the granule size could enhance bone regeneration. The advancement of bone formation by 53- to 300-μm OCP/Col resulted in fusion of new bone that could be nucleated from the OCP granules within Col matrix.

XRD analysis of the retrieved tissue with OCP/Col implants indicated that OCP tends to convert to HA until 12 weeks after implantation, although XRD showed the remnant OCP unresorbed and the newly formed bone.[23] The conversion from OCP to HA induces physicochemical changes with advancement of the conversion[5,19,45] and enhances osteoblastic differentiation of mouse bone marrow stromal cells together with an increase in differentiation markers, such as alkaline phosphatase (ALP) and osterix messenger RNA, in *in vitro* analyses.[17-19,46] Therefore, the granules of OCP in OCP/Col in the present study may affect bone regeneration to some extent regardless of granule size. The dissolution test of OCP/Col in a medium indicated that calcium ions tended to decrease, whereas inorganic phosphate ions tended to increase with smaller granule size. The conversion from OCP to HA *in vitro* accompanied these changes in ion concentration.[5,17,45] On the other hand, the surface area of OCP granules in Col matrix should be greater with smaller granule size because the same weight of OCP granules is included in the unit volume of the Col. The decrease in DS with respect to HA and OCP in the medium with 53- to 300-μm OCP/Col suggests that the smallest OCP granules in Col tend to convert to HA more readily than the

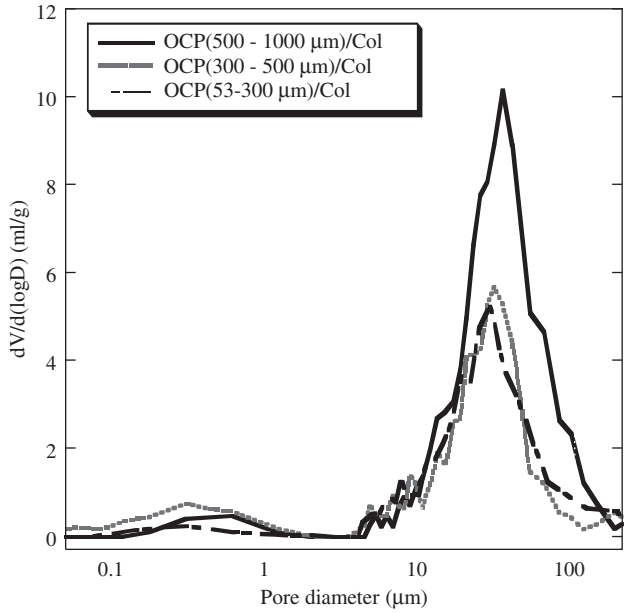

FIG. 9. Mercury porosimetry pore size distribution of 500- to 1,000-μm OCP/Col, 300 to 500-μm OCP/Col, and 53- to 300-μm OCP/Col.

larger granules. If the enhancement of the conversion from OCP to HA detected *in vitro* is reflected at the implantation site, then the stimulatory effect by the conversion from OCP to HA[19] might be involved in bone regeneration.

The resorption rate of OCP/Col was greater with smaller OCP granule size. As discussed above, one of reasons for earlier resorption could be the physicochemical factor that smaller granules of OCP are expected to have a higher specific surface area[28] in the unit volume in OCP/Col and, therefore, tend to dissolve faster than larger granules of OCP. Histochemical analysis revealed that TRAP staining was qualitatively higher in OCP/Col with smaller OCP granules than in that with larger granules. It has been proved that osteoclast formation can be induced on OCP coating from *in vitro* co-culturing in osteoblasts and bone marrow cells even in the absence of vitamin D_3, a factor to increase osteoclast-inducing factor RANKL in osteoblasts,[16] and that TRAP-positive osteoclast-like cells resorb OCP granules.[47,48] The present results reconfirmed that osteoclast-like cells can resorb OCP granules and suggest that decreasing the granule size of OCP enhances the osteoclastic cellular activity to resorb.

The effect of granule size in HA, β-TCP, and glass ceramics on bone formation has been seen in rabbit bone marrow.[49] It is becoming clear that the type of materials and granule size should be factors in the control of reactive bone formation.[9,10] HA is the most-thermodynamic stable basic salt in the physiological environment.[5] HA particles from 1 to 3 μm[49] or nano-HA deposited Col[12] have biodegradable properties if implanted in bone defects. The size of HA particles, ranging from submicron size to approximately 800 μm in diameter, affects the biological response to fibroblasts and myoblasts.[50] The size between the nano- and micrometer ranges also has an influence on osteoblast differentiation.[51] A previous histomorphometric analysis of mouse critical-sized calvaria defects revealed that OCP granules with the same granule size as those in the present study but not including the Col matrix enhanced bone formation and the appearance of TRAP-positive cells around OCP granules with larger OCP granule size; this is in contrast to the present results. In this previous study, it was easier for osteoblasts to invade, proliferate, and differentiate within the space formed by OCP granules by increasing granule size.[28] Although the effect of the granule size was opposite between the present (in the presence of Col) and previous (in the absence of Col) results,[28] the enhancement of bone regeneration was coupled with the increase in TRAP activity of osteoclast-like cells in these two observations. A similar coupling-like response to OCP granules has been found in rabbit bone marrow implantation[47] and mouse calvaria onlay graft,[52] suggesting that the enhancement of bone regeneration by OCP granules includes the activation of osteoclast-like cells around the granules during bone formation by osteoblasts. Furthermore, bone formation–related genes, such as osteocalcin, Col 1, osteopontin, and ALP, have been detected together with osteoclast-related genes, such as TRAP and Cathepsin-K in rat tibia bone marrow tissue with OCP implantation.[21]

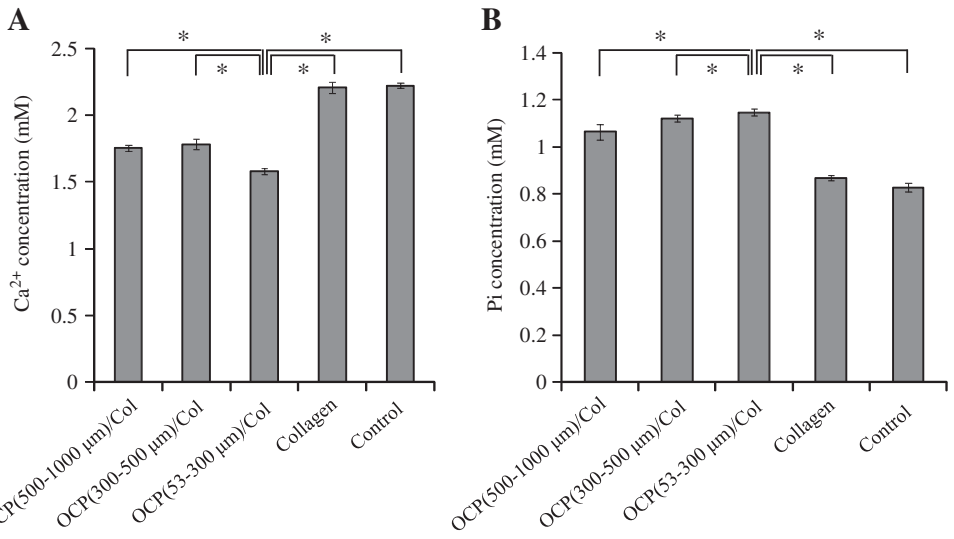

FIG. 10. Changes in the Ca^{2+} **(A)** and Pi **(B)** concentrations of alpha minimum essential medium at 37°C after 3 days of incubation of OCP/Col.

Table 1. Solution Composition and Its Saturation Levels after Incubation in αMEM.

Materials	Calcium (mM)	Phosphate (mM)	Degree of Supersaturation		
			HA	OCP	DCPD
OCP (500-1000 μm)/Col	1.76 ± 0.02	1.07 ± 0.03	3.11×10^{11}	1.04×10^{3}	5.51×10^{-1}
OCP (300-500 μm)/Col	1.78 ± 0.04	1.12 ± 0.01	3.85×10^{11}	1.27×10^{3}	5.87×10^{-1}
OCP (53-300 μm)/Col	1.58 ± 0.02	1.15 ± 0.01	2.34×10^{11}	8.69×10^{2}	5.38×10^{-1}
Collagen	2.21 ± 0.04	2.22 ± 0.02	5.27×10^{11}	1.39×10^{3}	5.62×10^{-1}
Control (Medium)	2.22 ± 0.02	0.83 ± 0.01	4.70×10^{11}	1.24×10^{3}	5.39×10^{-1}

Concentration of calcium and phosphate was expressed as average ± SD by three determinations.
αMEM, α minimal essential medium; HA, hydroxyapatite; OCP, octacalcium phosphate; DCPD, dicalcium phosphate dihydrate; col, collagen.

The present study using rat critical-sized calvaria showed that OCP/Col composite can be optimized for use in the repair of defects if a smaller OCP granule size (53-300 μm) is used in the composite. From the viewpoint of the quality of regenerated bone, complete resorption of OCP granules concomitantly with replacement with new bone may be desirable.[2] OCP granules in the present study were not resorbed fully and remained even when OCP/Col with the smallest granules was used and the implantation was conducted over prolonged periods. HA is the thermodynamically most-stable salt in various calcium phosphates,[5] so the converted HA from OCP should have lower solubility than the original OCP, as revealed in a previous *in vitro* study under physiological conditions.[45] Converted HA from an OCP onlay implanted in rat calvaria is carbonate-containing HA.[53] Carbonate-containing HA is thought to be an analogue to biological apatite crystals in bone[54-56] and, therefore, exhibits higher osteoclastic cellular resorbability.[11,57,58] The osteoclastic resorption of OCP/Col composite is remarkably accelerated under mechanical conditions *in vivo*[53,59] and *in vitro*.[59] Alleviation of the mechanical stress reduces this marked osteoclastic activity, resulting in restoring the bone-regenerative property.[59] The use of a OCP/Col composite in a load-bearing site is therefore challenging. The acquisition of the ability to be fully resorbed and replaced with new bone in various implantation sites is a problem to be solved from the materials science and chemistry viewpoints and would lead to the development of an OCP-based bone substitute material that is compatible with autologous bone.

Conclusion

The present study showed that the granule size of OCP can modify the bone regenerative property of a bone substitute material consisting of OCP granules and a Col matrix. Decreasing the OCP granule size to 53 to 300 μm in a OCP/Col composite enhanced its capability to regenerate new bone relative to the larger sizes of OCP. The physicochemical property induced by the difference of the granule size may be a determinant of the bone regenerative property of OCP/Col. It appears that bone regeneration is coupled with enhanced osteoclastic resorption of OCP granules in OCP/Col. Recent studies clarified that OCP exhibits a variety of biological responses depending on the crystal chemistry.[21,48] The present study provides a clue to increase the osteoconductivity of OCP/Col by stimulating host osteoblastic cells, leading to the development of a highly osteoconductive bone substitute material and a scaffold for a tissue construct with exogenous cells approaching the performance of autologous bone.

Acknowledgments

This study was supported in part by grants in aid 17076001, 19390490, 23390450, 23659999, and 23106010 from the Ministry of Education, Science, Sports, and Culture of Japan and the Suzuken Memorial Foundation.

Disclosure Statement

No conflicting financial interests exist.

References

1. Tamai, N., Myoui, A., Tomita, T., Nakase, T., Tanaka, J., Ochi, T., and Yoshikawa, H. Novel hydroxyapatite ceramics with an interconnective porous structure exhibit superior osteoconduction in vivo. J Biomed Mater Res **59**, 110, 2002.
2. Ghanaati, S., Barbeck, M., Orth, C., Willershausen, I., Thimm, B.W., Hoffmann, C., Rasic, A., Sader, R.A., Unger, R.E., Peters, F., and Kirkpatrick, C.J. Influence of beta-tricalcium phosphate granule size and morphology on tissue reaction in vivo. Acta Biomater **6**, 4476, 2010.
3. LeGeros Rz. Properties of osteoconductive biomaterials: calcium phosphates. Clin Orthop **72**, 81, 2002.
4. Ogose, A., Hotta, T., Kawashima, H., Kondo, N., Gu, W., Kamura, T., and Endo, N. Comparison of hydroxyapatite and beta tricalcium phosphate as bone substitutes after excision of bone tumors. J Biomed Mater Res B Appl Biomater **72**, 94, 2005.
5. Brown WE, Mathew M, and Tung MS. Crystal chemistry of octacalcium phosphate. Prog Cryst Growth Charact **4**, 59, 1981.
6. Chow L. Solubility of calcium phosphates. In: Chow, L.C., and Eanes, E.D. Octacalcium Phosphate. Basel, Switzerland: Karger, 2001, pp. 94–111.
7. Bucholz RW. Nonallograft osteoconductive bone graft substitutes. Clin Orthop **395**, 44, 2002.
8. Papangkorn, K., Yan, G., Heslop, D.D., Moribe, K., Baig, A.A., Otsuka, M., and Higuchi, W.I. Influence of crystallite microstrain on surface complexes governing the metastable equilibrium solubility behavior of carbonated apatites. J Colloid Interface Sci **320**, 96, 2008.
9. Okuda, T., Ioku, K., Yonezawa, I., Minagi, H., Gonda, Y., Kawachi, G., Kamitakahara, M., Shibata, Y., Murayama, H., Kurosawa, H., and Ikeda, T. The slow resorption with replacement by bone of a hydrothermally synthesized pure calcium-deficient hydroxyapatite. Biomaterials **29**, 2719, 2008.
10. Okuda, T., Ioku, K., Yonezawa, I., Minagi, H., Kawachi, G., Gonda, Y., Murayama, H., Shibata, Y., Minami, S., Kamihira, S., Kurosawa, H., and Ikeda, T. The effect of the microstructure of beta-tricalcium phosphate on the metabolism of subsequently formed bone tissue. Biomaterials **28**, 2612, 2007.

11. Okazaki, M., Ohmae, H., Takahashi, J., Kimura, H., and Sakuda, M. Insolubilized properties of UV-irradiated CO_3 apatite-collagen composites. Biomaterials **11**, 568, 1990.
12. Kikuchi, M., Itoh, S., Ichinose, S., Shinomiya, K., and Tanaka, J. Self-organization mechanism in a bone-like hydroxyapatite/collagen nanocomposite synthesized in vitro and its biological reaction in vivo. Biomaterials **22**, 1705, 2001.
13. Brown, W.E., Smith, J.P., Lehr, J.R., and Frazier, A.W.. Crystallographic and chemical relations between octacalcium phosphate and hydroxyapatite. Nature **196**, 1050, 1962.
14. Bohner, M. Resorbable biomaterials as bone graft substitutes. Materials Today **13**, 24, 2010.
15. Suzuki, O., Imaizumi, H., Kamakura, S., and Katagiri, T. Bone regeneration by synthetic octacalcium phosphate and its role in biological mineralization. Curr Med Chem **15**, 305, 2008.
16. Takami, M., Mochizuki, A., Yamada, A., Tachi, K., Zhao, B., Miyamoto, Y., Anada, T., Honda, Y., Nakamura, M., Suzuki, O., and Kamijo, R. Osteoclast differentiation induced by synthetic octacalcium phosphate through RANKL expression in osteoblasts. Tissue Eng Part A **15**, 3991, 2009.
17. Anada, T., Kumagai, T., Honda, Y., Masuda, T., Kamijo, R., Kamakura, S., Yoshihara, N., Kuriyagawa, T., Shimauchi, H., and Suzuki, O. Dose-dependent osteogenic effect of octacalcium phosphate on mouse bone marrow stromal cells. Tissue Eng **14**, 965, 2008.
18. Shelton, R.M., Liu, Y., Cooper, P.R., Gbureck, U., German, M.J., and Barralet, J.E. Bone marrow cell gene expression and tissue construct assembly using octacalcium phosphate microscaffolds. Biomaterials **27**, 2874, 2006.
19. Suzuki, O., Kamakura, S., Katagiri, T., Nakamura, M., Zhao, B., Honda, Y., and Kamijo, R. Bone formation enhanced implanted octacalcium phosphate involving conversion into Ca-deficient hydroxyapatite. Biomaterials **27**, 2671, 2006.
20. Kamakura, S., Sasano, Y., Shimizu, T., Hatori, K., Suzuki, O., Kagayama, M., and Motegi, K. Implanted octacalcium phsphate is more resorbable than beta-tricalcium phosphate and hydroxyapatite. J Biomed Mater Res **59**, 29, 2002.
21. Miyatake, N., Kishimoto, K.N., Anada, T., Imaizumi, H., Itoi, E., and Suzuki, O. Effect of partial hydrolysis of octacalcium phosphate on its osteoconductive characteristics. Biomaterials **30**, 1005, 2009.
22. Suzuki, O., Nakamura, M., Miyasaka, Y., Kagayama, M., and Sakurai, M. Bone formation on synthetic precursors of hydroxyapatite. Tohoku J Exp Med **164**, 37, 1991.
23. Kamakura, S., Sasaki, K., Honda, Y., Anada, T., and Suzuki, O. Octacalcium phosphate combined with collagen orthotopically enhances bone regeneration. J Biomed Mater Res B Appl Biomater **79**, 210, 2006.
24. Fuji, T., Anada, T., Honda, Y., Shiwaku, Y., Koike, H., Kamakura, S., Sasaki, K., and Suzuki, O. Octacalcium phosphate-precipitated alginate scaffold for bone regeneration. Tissue Eng Part A **15**, 3525, 2009.
25. Williams, D.F. On the mechanisms of biocompatibility. Biomaterials **29**, 2941, 2008.
26. Rezwan, K., Chen, Q.Z., Blaker, J.J., and Boccaccini, A.R. Biodegradable and bioactive porous polymer/inorganic composite scaffolds for bone tissue engineering. Biomaterials **27**, 3413, 2006.
27. Bonfield, W. Designing porous scaffolds for tissue engineering. Philos Transact A Math Phys Eng Sci **364**, 227, 2006.
28. Murakami, Y., Honda, Y., Anada, T., Shimauchi, H., and Suzuki, O. Comparative study on bone regeneration by synthetic octacalcium phosphate with various granule sizes. Acta Biomater **6**, 1542, 2010.
29. Kawai, T., Anada, T., Honda, Y., Kamakura, S., Matsui, K., Matsui, A., Sasaki, K., Morimoto, S., Echigo, E., and Suzuki, O. Synthetic octacalcium phosphate augments bone regeneration correlated with its content in collagen scaffold. Tissue Eng Part A **15**, 23, 2009.
30. Suzuki, O., Nakamura, M., Miyasaka, Y., Kagayama, M., and Sakurai, M. Maclura pomifera agglutinin-binding glycoconjugates on converted apatite from synthetic octacalcium phosphate implanted into subperiosteal region of mouse calvaria. Bone Miner **20**, 151, 1993.
31. Suzuki, O., Yagishita, H., Amano, T., and Aoba, T. Reversible structural changes of octacalcium phosphate and labile acid phosphate. J Dent Res **74**, 1764, 1995.
32. Fowler, B.O., Moreno, E.C., and Brown, W.E. Infra-red spectra of hydroxyapatite, octacalcium phosphate and pyrolysed octacalcium phosphate. Arch Oral Biol **11**, 477, 1966.
33. Nelson, D.G., and McLean, J.D. High-resolution electron microscopy of octacalcium phosphate and its hydrolysis products. Calcif Tissue Int **36**, 219, 1984.
34. Aoba, T., and Moreno, E.C. The enamel fluid in the early secretory stage of porcine amelogenesis: chemical composition and saturation with respect to enamel mineral. Calcif Tissue Int **41**, 86, 1987.
35. Moreno, E.C., and Aoba, T. Calcium bonding in enamel fluid and driving force for enamel mineralization in the secretory stage of amelogenesis. Adv Dent Res **1**, 245, 1987.
36. Moreno, E.C., and Aoba, T. Comparative solubility study of human dental enamel, dentin, and hydroxyapatite. Calcif Tissue Int **49**, 6, 1991.
37. Moreno, E.C., Kresak, M., and Zahradnik, R.T. Physicochemical aspects of fluoride-apatite systems relevant to the study of dental caries. Caries Res **11 Suppl 1**, 142, 1977.
38. Moreno, E.C., Brown, W.E., and Osborn, G. Stability of dicalcium phosphate dehydrate in aqueous solutions and solubility product of octacalcim phosphate. Soil Sci Soc Am Proc **24**, 99, 1960.
39. Mathew, M., Brown, W.E., Schroeder, L.W., and Dickens, B. Crystal structure of octacalcium bis(hydrogenphosphate) tetrakis(phosphate)pentahydrate, $Ca_8(HPO_4)_2(PO_4)_4 \cdot 5H_2O$. J Crystallogr Spectrosc Res **18**, 235, 1988.
40. Kamakura, S., Sasaki, K., Honda, Y., Anada, T., Matsui, K., Echigo, S., and Suzuki, O. Dehydrothermal treatment of collagen influences on bone regeneration by octacalcium phosphate (OCP) collagen composites. J Tissue Eng Regen Med **1**, 450, 2007.
41. Wang, M.C., Pins, G.D., and Silver, F.H. Collagen fibres with improved strength for the repair of soft tissue injuries. Biomaterials **15**, 507, 1994.
42. Weadock, K.S., Miller, E.J., Bellincampi, L.D., Zawadsky, J.P., and Dunn, M.G. Physical crosslinking of collagen fibers: comparison of ultraviolet irradiation and dehydrothermal treatment. J Biomed Mater Res **29**, 1373, 1995.
43. Kamakura, S., Sasano, Y., Homma, H., Suzuki, O., Kagayama, M., and Motegi, K. Implantation of octacalcium phosphate (OCP) in rat skull defects enhances bone repair. J Dent Res **78**, 1682, 1999.
44. Geiger, M., Li, R.H., and Friess, W. Collagen sponges for bone regeneration with rhBMP-2. Adv Drug Deliv Rev **55**, 1613, 2003.
45. Suzuki, O., Kamakura, S., and Katagiri, T. Surface chemistry and biological responses to synthetic octacalcium phosphate. J Biomed Mater Res Appl Biomater **77B**, 201, 2006.
46. Liu, Y., Cooper, P.R., Barralet, J.E., and Shelton, R.M. Influence of calcium phosphate crystal assemblies on the

proliferation and osteogenic gene expression of rat bone marrow stromal cells. Biomaterials **28**, 1393, 2007.
47. Imaizumi, H., Sakurai, M., Kashimoto, O., Kikawa, T., and Suzuki, O. Comparative study on osteoconductivity by synthetic octacalcium phosphate and sinterd hydroxyapatite in rabbit bone marrow. Calcif Tissue Int **78**, 45, 2006.
48. Honda, Y., Anada, T., Kamakura, S., Morimoto, S., Kuriyagawa, T., and Suzuki, O. The effect of microstructure of octacalcium phosphate on the bone regenerative property. Tissue Eng Part A **15**, 1965, 2009.
49. Oonishi, H., Hench, L.L., Wilson, J., Sugihara, F., Tsuji, E., Kushitani, S., and Iwaki, H. Comparative bone growth behavior in granules of bioceramic materials of various sizes. J Biomed Mater Res **44**, 31, 1999.
50. Sun, J.-S., Tsuang, Y.-H., Chang, W.H.-S., Li, J., Liu, H.-C., and Lin, F.-H. Effect of hydroxyapatite particle size on myoblasts and fibroblasts. Biomaterials **18**, 683, 1997.
51. Liu, H., Yazici, H., Ergun, C., Webster, T.J., and Bermek, H. An in vitro evaluation of the Ca/P ratio for the cytocompatibility of nano-to-micron particulate calcium phosphates for bone regeneration. Acta Biomater **4**, 1472, 2008.
52. Kikawa, T., Kahimoto, O., Imaizumi, H., Kokubun, S., and Suzuki, O. Intramembranous bone tissue response to biodegradable octacalcium phosphate implant. Acta Biomater **5**, 1756, 2009.
53. Suzuki, Y., Kamakura, S., Honda, Y., Anada, T., Hatori, K., Sasaki, K., and Suzuki, O. Appositional bone formation by OCP-collagen composite. J Dent Res **88**, 1107, 2009.
54. Brown, W.E. Crystal growth of bone mineral. Clin Orthop Rel Res **44**, 205, 1966.
55. Simpson, D.R. Problems of the composition and structure of the bone minerals. Clin Orthop Rel Res **86**, 260, 1972.
56. Young, R.A. Implications of atomic substitutions and other structural details in apatites. J Dent Res **53**, 193, 1974.
57. Doi, Y., Iwanaga, H., Shibutani, T., Moriwaki, Y., and Iwayama, Y. Osteoclastic responses to various calcium phosphates in cell cultures. J Biomed Mater Res **47**, 424, 1999.
58. Spence, G., Patel, N., Brooks, R., Bonfield, W., and Rushton, N. Osteoclastogenesis on hydroxyapatite ceramics: The effect of carbonate substitution. J Biomed Mater Res Part A **92A**, 1292, 2010.
59. Matsui, A., Anada, T., Masuda, T., Honda, Y., Miyatake, N., Kawai, T., Kamakura, S., Echigo, S., and Suzuki, O. Mechanical stress-related calvaria bone augmentation by onlayed octacalcium phosphate-collagen implant. Tissue Eng Part A **16**, 139, 2010.

Address correspondence to:
Osamu Suzuki, Ph.D., M.Eng.
Division of Craniofacial Function Engineering
Tohoku University Graduate School of Dentistry
4-1 Seiryo-machi
Aoba-ku, Sendai 980-8575
Japan

E-mail: suzuki-o@m.tohoku.ac.jp

Received: June 19, 2011
Accepted: September 21, 2011
Online Publication Date: October 31, 2011